Simultaneous reception of body coil and surface coil array data for intensity-corrected self-calibrated parallel MRI

M. A. Ohliger[1], S. V. Suddarth[1], A. K. Grant[1], T. Niendorf[1,2], D. K. Sodickson[1]

[1]Radiology, Beth Israel Deaconess Medical Center, Boston, MA, United States, [2]Applied Sciences Laboratory, GE Heathcare Technologies, Boston, MA, United States

Introduction. Self-calibrated parallel MRI techniques (1-4) combine undersampled acquisitions of the outer regions of k-space together with fully-sampled acquisitions of the central regions of k-space. The fully-sampled central lines provide low resolution images that are used as coil array calibration information. Self-calibrated techniques are valuable because they eliminate the need for independent sensitivity reference scans and they also reduce reconstruction artifacts that can occur when the coil sensitivities of the reference scan do not exactly match those of the acquired data.

The coil reference images that are extracted from the central k-space positions of a self-calibrated acquisition are modulated by low-resolution components of the sample magnetization. These data contain information about the relative reception profiles of different array elements, but they generally do not provide information about the absolute coil sensitivity functions. As a result, the reconstructed images are typically also modulated by the intensity profile of the surface coils. While this intensity modulation does not impact the SNR of the image, it can interfere with quantitative interpretations of MR data and degrade the subjective impressions of image quality.

In this study, we present a technique for the acquisition of intensity-corrected self-calibrated parallel MRI data. Intensity correction is achieved by acquiring data with the MRI body coil simultaneously with the surface array coils. Even for externally-calibrated data, this technique eliminates the need for a separately-acquired body coil image, which is normally necessary when intensity correction is required.

Theoretical formulations of parallel reconstructions such as SENSE (5) guarantee that additional coil elements can be incorporated into the reconstructions with no loss in SNR. There may be concern, however, that inductive coupling between the surface coils and the body coil during simultaneous acquisition might potentially reduce image quality. At the same time, it has been shown that for non-parallel MRI data and a 3-coil array, the simultaneous acquisition of body coil data causes little change in image SNR when compared to the array coils alone (6). In addition, it has been suggested that small amounts of inductive coupling may not be problematic for parallel MRI (7). Besides inductive coupling, there is also concern that the relatively low SNR of the body coil sensitivity might introduce additional noise into the reconstructed image.

Materials and Methods: ***Image Acquisition***. All images were acquired using a 1.5 T TwinSpeed MRI scanner (*GE Healthcare Technologies, Waukesha Wisconsin*). Body coil and array coils were acquired simultaneously using two receiver cabinets that were in a synchronized master-slave configuration, similar to the four sets of electronics that were used in (8). The master cabinet, which was also responsible for RF excitation and gradient switching, was run in standard "body coil" mode. The slave cabinet, which contained eight receiver channels, was configured in array coil mode and was responsible for receiving the array data. Custom-built PIN-diode drivers were used to bypass the coil element bias signals that would normally be provided by the master for the array coils. Note that this relatively complex multi-cabinet arrangement, which we used because of availability at our institution, could be simplified by appropriate system software changes allowing simultaneous body coil and array reception

An imaging phantom was placed at the magnet's isocenter, and it was surrounded by eight surface coils (*Nova Medical, Inc. Wilmington MA)*. Each coil element measured 8x18 cm, and was connected to the system through a specialized low-impedance preamplifier. Fully-sampled axial images were obtained using a 3D spoiled gradient echo pulse sequence (32 slices, slice thickness=6 mm, FOV=40 cm, matrix 128x128, TE=1.7 ms, TR=4.6 ms, α=10, BW=+/-32.5 KHz, phase encode LR). Identical data sets were acquired using 1) the scanner's body coil alone, 2) the array coil alone, and 3) the body coil and the array together. Self-calibrated data were created by extracting one out of every three lines from the outer parts of k-space and leaving the 20 full-sampled lines at the center of k-space, yielding a net acceleration factor of 2.3.

Image Reconstruction. Although the technique presented here is compatible with any self-calibrated image reconstruction technique, we followed the general procedure outlined in Ref (2). In this approach, the variable-density acquisition is reconstructed by placing sensitivity variations and gradient modulations together into an encoding matrix, which is inverted in order to reconstruct the fully-sampled image. When the central k-space lines are used as reference images, the encoding matrix (and thus the reconstruction matrix) is modulated by the low-resolution components of the magnetization density (Ref. (2), Eq. [11]). These low-resolution modulations are removed by post-multiplying the encoding-matrix inverse by a sum-of-squares combination of the reference images (Ref. (2), Eq. [13]). In this case, the reconstruction algorithm yields a full-resolution image that is modulated by the sensitivity variations of the surface coils. In the present technique, however, we recognize that if body coil data are acquired simultaneously with array coil data, then the sum-of-squares post-multiplication of Ref. (2), Eq. [13], can be replaced by a simple post-multiplication by the acquired body coil sensitivity: $\mathbf{I}^{reconstructed}(\mathbf{r}) = \mathbf{I}^{reference}_{body}\rho^{recon}(\mathbf{r}) = \mathbf{I}^{reference}_{body}\rho\ (\mathbf{r}) / \rho^{low-res}(\mathbf{r}) = C^{\text{body coil}}(\mathbf{r})\rho\ (\mathbf{r})$.

FIGURE 1

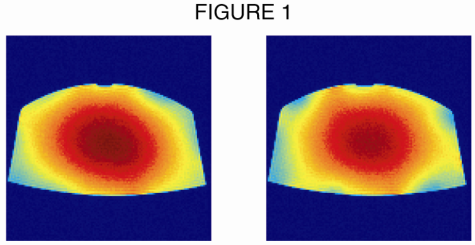

a. body coil image surface array deactivated — b. body coil image surface array activated

FIGURE 2

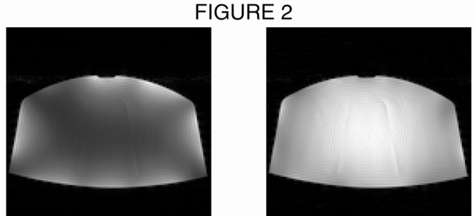

a. without body coil — b. with body coil

Results Figure 1 shows the central axial slice through a phantom acquired using the body coil (a) with the surface coils deactivated and (b) with the surface coils acquiring data. The body coil shows moderate evidence of signal coupling immediately underneath the surface coils, but the intensity profile of the body coil throughout the phantom is largely unchanged.

Figure 2 shows the results of self-calibrated reconstructions of the central slice of the phantom. (a) was acquired with the surface array alone, and (b) was acquired with the surface array combined with the body coil. The acquisition and reconstruction that incorporates the body coil clearly shows a more uniform sensitivity profile.

Discussion We have demonstrated the feasibility of acquiring self-calibrated parallel MRI data simultaneously with a surface coil array and the uniform-sensitivity body coil. The body coil image distribution is minimally changed by the simultaneous acquisition of surface coil data. As a consequence, it is possible to compensate for surface coil sensitivity variations in self-calibrated parallel MRI data. While further experiments are necessary to determine the precise impact of this simultaneous acquisition on the SNR of the reconstructed images, the results presented here suggest that there is a potentially powerful role for incorporating body coil data directly into parallel imaging reconstructions. The simultaneous acquisition of body coil and surface coil data can also potentially improve the quantification of spectroscopic data.

Ref: 1) Jakob *et al* MAGMA 7:42-54 2) McKenzie *et al* MRM 47:529-538 3) Griswold *et al* MRM 47:1202-1210 4) Yeh *et al* ISMRM 2002 p. 2390 5) Pruessmann *et al* MRM 42:952-962 6) Kochrain *et al* 44:660-663 7) Ohliger *et al* MEM 52:628-639 8) Zhu *et al* MRM 52:869-877